Advances in Sintering Science and Technology II

Edited by

Suk-Joong L. Kang

Rajendra Bordia

Eugene Olevsky

Didier Bouvard

Ceramic Transactions

Volume 232

WILEY

The American Ceramic Society

Advances in Sintering Science and Technology II

Advances in Sintering Science and Technology II

Ceramic Transactions, Volume 232

A Collection of Papers Presented at The International Conference on Sintering 2011, August 28—September 1, Jeju, Korea

Edited by
Suk-Joong L. Kang
Rajendra Bordia
Eugene Olevsky
Didier Bouvard

WILEY

A John Wiley & Sons, Inc., Publication

Published by John Wiley & Sons, Inc., Hoboken, New Jersey.
Published simultaneously in Canada.

Library of Congress Cataloging-in-Publication Data is available.

ISBN: 978-1-118-27375-3
ISSN: 1042-1122

Printed in the United States of America.

10 9 8 7 6 5 4 3 2 1

Contents

MICROSTRUCTURAL EVOLUTION AND PHYSICAL PROPERTIES

UNCONVENTIONAL SINTERING PROCESSES

Preface

This issue of the Ceramic Transactions includes a number of papers presented at the International Conference on Sintering 2011, which was held on Jeju Island, Republic of Korea, on August 26—September 1, 2011. The meeting was chaired by Professors Suk-Joong L. Kang, Rajendra Bordia, Eugene Olevsky, and Didier Bouvard.

This was the sixth meeting in a series that started in 1995 as a continuation of the well-known cycle of conferences on sintering and related phenomena organized by G. Kuczynski which ran from 1967 to 1983. The first five meetings in this reestablished series of conferences were held at Pennsylvania State University in 1995, 1999 and 2003; in Grenoble, France in 2005; and in San Diego, California in 2008.

Sintering 2011 brought together more than 260 participants from 27 countries, fostering a high level of scientific interaction and creating an atmosphere of broad international collaboration. The meeting included participants from North and Central America, Europe (both Eastern and Western), Asia, Australia and Africa.

The conference demonstrated the advances that have been made in the areas of the multi-scale modeling of densification and in microstructure development and promoted a better understanding of the processing of complex systems (multi-layered, composite and reactive systems). Concerning sintering technology, innovative approaches such as field-assisted sintering attracted the attention of the materials processing community. Other timely topics included the sintering and microstructural development of nanostructured materials, and the sintering of bio- and energy applications-related materials.

Twenty five papers of Sintering 2011 authors were published in special issues of the Journal of the American Ceramic Society and of the Journal of Materials Science (July 2011). The American Ceramic Society is publishing approximately 20 papers presented at this meeting in this volume of the Ceramic Transactions. Together, these forty five papers cover the rich diversity of the sintering science and technology topics, which were presented at the conference. Both the conference participants and organizers had to meet numerous deadlines to enable the timely

publication of this volume and of the special issues of the Journal of the American Ceramic Society and of the Journal of Materials Science.

We hope that this collection of articles will be an important contribution to the literature, and we are looking forward to seeing you at future Sintering conferences.

SUK-JOONG L. KANG, RAJENDRA BORDIA, EUGENE OLEVSKY, AND DIDIER BOUVARD
Sintering 2011 Co-Chairs

Powder Synthesis and Sintering

DEPOSITION OF PLATINUM NANOPARTICLES ONTO COPPER FOILS BY ELECTROPHORESIS: A STUDY OF THE SINTERING DYNAMICS AT THE PLATINUM-COPPER INTERFACE

Deborah C. Blaine*, Alexander Ilchev†, Leslie Petrik†, Patrick Ndungu‡, and Alexander Nechaev†

*Mechanical and Mechatronics Engineering, Stellenbosch University, South Africa
†Environmental Nanosciences, University of the Western Cape, South Africa
‡Department of Chemistry, University of KwaZulu-Natal, South Africa

ABSTRACT

The effect of decreasing the size of platinum to the nanoscale for the copper-platinum alloy system was investigated while coupled to the research on the electrophoresis of platinum nanoparticles. It was observed that the temperature for the nanoPt-Cu eutectoid transformation decreased to 300°C compared to the value of 418°C for a bulk Pt-Cu system. HRTEM and XRD results showed that sintering between the Pt nanoparticles and copper surface begins at temperatures as low as 200°C. Surface diffusion was dominant at 200°C while bulk diffusion became dominant at 300°C, at which stage the sintered product had formed a tri-phasic system of pure copper, Pt-Cu alloy and Pt nanoparticles which were sintered to the alloy. No platinum nanoparticles remained after sintering at 400°C, having all diffused into the Pt-Cu alloy. Sintering above 300°C saw the appearance of the Cu_3Pt phase. HRTEM imaging of the particles found that there was an increase in particle size from 2.5 nm at 25°C to 0.5 microns at 400°C. These results were compared to particle size calculations using XRD measurements. The particle geometry changed from spherical at 25°C to cubic at and above 300°C.

INTRODUCTION

Nanotechnology is defined as any technology performed on a nanoscale that has applications in the real world.[1] It encompasses any device, natural or synthetic, that has at least one of its dimensions on the length scale of 0.1 – 100 nm. Such devices include thin films, nanolayered materials and membranes (one dimension on the nanoscale), nanotubes, nanorods, nanowires and nanofibres (two dimensions on the nanoscale), as well as nanoparticles, nanospheres, quantum dots, micelles and dendrimers (all three dimensions on the nanoscale.) These are the basic building blocks in nanotechnology and the integration of such components is the basis for the design of nanostructured systems. Perhaps the most exciting discovery in this field was the quantum size effect[1] where as a material's dimensions are reduced to the nanoscale, its properties begin to gradually shift from those of the bulk to novel ones which are better explained by quantum mechanics. Understanding the parameters which control the synthesis outcome and inherent properties of these components allows for the tailoring of novel technological devices which allow the fantastic idea of being able to control chemical systems, on a molecular or even atomic level, to come to life.

The use and development of platinum based materials is becoming ever more crucial in modern technology each day. The application of platinum and its alloys in the field of heterogeneous catalysis is well known and, in many cases, held as a standard. Fuel cell research, as well as other aspects of the hydrogen economy, is mostly based on developing such materials.[2] Additionally, catalytic converters, used to reduce emissions in automobiles and for catalytic cracking in the petroleum industry, have been dependant on platinum alloys since their commercialisation.[3] Other application for platinum in the catalysis industry include the production of chemicals, such as nitric acid[4], hydrogen cyanide[5] and various others hydrocarbons relevant to the petrochemical industry.[6,7]

The selectivity and activity of each process can be modified by using alloys of the different precious metals with each other and/or with other transition metals.[8, 9] Work by both Chandler *et al.*[10] as well as Weihua *et al.*[11] have shown that Pt-Cu bimetallic nanoparticles also show superior catalytic

properties compared to pure platinum. Koh *et al.*[12] and Mani *et al.*[13] both reported on the development of dealloyed Pt-Cu nanoparticles with a near-surface alloy structure as well as a high degree of porosity which not only improved catalyst performance by up to 4 times that of commercial Pt-C but also improved catalyst tolerance to poisoning. Pure platinum has shown poor performance as a catalyst for the oxygen reduction reaction (ORR). The reduction of oxygen in aqueous media by platinum catalysts has been extensively studied for application in fuel cells by Antolini *et al.*[9,14], Bell[15], Luo *et al.*[16,17], Regalbuto[18], Koh *et al.*[12], Mani *et al.*[13] as well as Wang *et al.*[19]. They have shown that binary alloys of platinum with other metals such as cobalt, chromium, vanadium, titanium and copper has shown a marked increase in catalytic activity towards the oxygen reduction reaction.

Van der Biest *et al.*[20] as well as Bersa *et al.*[21] stated that EPD has been successfully employed in the formation of wear-resistant and anti-oxidant coatings, functional films in microelectronic devices and solid oxide fuel cells, membranes, sensors as well as composite and bioactive coatings for medical implants. Teranishi *et al.*[22] prepared 2D nanoarrays of platinum nanoparticles on carbon coated copper grids using EPD. Very little work exists for the EPD of platinum[22-25] hence this research offers insight into possible novel applications for the EPD process of platinum.

By developing a better understanding of the sintering dynamics of the Pt-Cu biphasic system, novel processes for the self-assembly of superior materials of the types mentioned above could be designed. The goal in this research was to determine the effects that reducing the platinum phase to the nanoscale had on the properties of the system.

Abe *et al.*[26] reported that for this system, a eutectoid transformation occurs at 418°C. In theory, reducing either of the phases to the nanoscale would decrease this limit for eutectoid formation. The parameters controlling the formation of CuPt and Cu_3Pt alloys as well as the diffusion characteristics between the Pt and Cu phases was considered by developing a two phase system with a defined boundary between each phase. This was achieved by depositing the platinum nanophase onto a copper foil using electrophoretic deposition (EPD).

EXPERIMENTAL PROCEDURES

Pt Nanoparticle Synthesis and Dispersion

A dispersion of platinum nanoparticles was prepared by the ethylene glycol method[27]. To prepare 200 ml of Pt nanoparticles dispersed in a 1:1 (v/v) mixture of anhydrous acetone and ethanol (AcEt), the following procedure was applied: 1g of NaOH (25 mmol) was dissolved in 50 ml of ethylene glycol (EtGly) at 100°C under N_2. 1g of H_2PtCl_6 (2.44 mmol) was also dissolved in 50 ml of EtGly at room temperature under nitrogen. The two solutions were then mixed together, heated up to 160°C under nitrogen and allowed to react with constant stirring for 2 hours. Once the reaction was complete, 100 ml of ultrapure water was added followed by 25 ml of 1M HCl. The mixture was centrifuged for 30 minutes at 5000 rpm after which the supernatant liquid was discarded. Thereafter, 200 ml of ultrapure water as well as 10 ml of 1M HCl was added to the precipitate, the mixture was shaken well to redisperse the platinum particles. The dispersion was centrifuged again for the same time at the same speed. After centrifugation, the supernatant liquid was discarded again and the platinum precipitate was redispersed in 200 ml of AcEt.

Copper Electrode Preparation

Copper electrodes for the EPD process, with dimensions of 50 mm × 10 mm, were cut from a 5.5 g copper foil of 0.25 mm thickness (supplier: Sigma Aldrich). The copper foil was sanded, sequentially, with 400 grit followed by 600 grit SiC paper,using an active oxide suspension (Struers OP-S suspension), and then polished using cotton wool only, soaked in the suspension. The electrodes were then rinsed with ultrapure water, followed by acetone and finally they were immersed in acetone and sonicated for 15 minutes. The electrodes were then dried with cotton wool.

Electrophoretic Deposition of the Pt Nanoparticles

The EPD apparatus consisted of a DC power supply (supplier: TDK-Lambda, model: Genesys™ GEN600:1.3, 0-600 Volts DC and 0-1.3 Amps DC range, 72 mV and 0.26 mA accuracy) which was connected to a cylindrical brass anode holder and a hollow, cylindrical, stainless steel cathode. The electrodes were housed in a Pyrex container so that the anode rested inside the cathode. Figure 1 shows a schematic diagram of EPD cell.

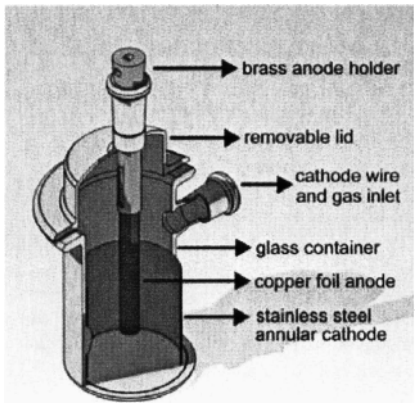

Figure 1. Schematic of the EPD cell.

A set of trials was performed to determine the deposition flux as a function of voltage and deposition time. Each trial was performed in air and 25 ml of the platinum dispersion at a concentration of 1.8 g/l was used. 12 trials with a potential range of 2 – 10 volts and a time range of 5 – 30 minutes were performed to gain an understanding of the deposition kinetics for the system. Table 1 gives the EPD parameters tested.

Table 1 Pt nanoparticle deposition flux at different EPD trial parameters: time at voltage

Deposition time (mins)	Deposition flux (mg/mm^2)		
5	0.0118	0.0210	0.0254
10	0.0150	0.0235	0.0314
20	0.0192	0.0257	0.0327
30	0.0200	0.0259	0.0331
Deposition voltage (V)	2	5	10

To prepare a sample deposit for sintering, 100 ml of the platinum dispersion was diluted with an equal volume of acetone. This dispersion, at a concentration of 0.9 g/l, was then used in the EPD cell to deposit the platinum nanoparticles as a film on the copper foil electrode. The cell was set to an applied voltage of 5 V and deposition occurred for 10 minutes.

Sintering the Pt Deposits

Sintering of the deposits was achieved in a vertical tube furnace. The copper electrode, onto which the Pt nanoparticles had been deposited, was suspended at the mouth of the furnace with a tungsten wire which ran through the furnace. The furnace was heated to the required temperature while being purged by argon gas. The electrode was then hoisted into the furnace with the tungsten wire and kept under flowing argon while the sintering took place. After 15 minutes, the furnace was rapidly purged with argon while the electrode was lowered out of the furnace. Deposit samples were sintered at 100°C, 200°C, 300°C and 400°C.

RESULTS

Synthesis of the Dispersed Pt Nanoparticles

The dispersion prepared was analyzed by HRTEM (high resolution transmission electron microscopy) using a Tecnai F20 field emission transmission electron microscope with coupled EDX (energy dispersive x-ray spectroscopy) capabilities, and XRD (X-ray diffraction) analysis using a PANalytical X'Pert Pro multipurpose diffractomator. The JCPDS (Joint Committee on Powder Diffraction Standards) database was used to characterize the XRD data collected.

The concentration of Pt in dispersion was measured as follows. Three 10 ml samples of the dispersion were each placed in pre-weighed glass vials. The mass of the dispersion in each sample was calculated by weighing the vials after the samples were added. Thereafter, the solvent was evaporated and the vials holding the precipitate only were weighed. The mass of the precipitate multiplied by 100 gives the concentration (in grams per litre) of Pt in the dispersion. The average concentration was taken as the concentration of Pt in the dispersion.

Figure 2(a) shows the HRTEM image of the Pt nanoparticles synthesized by the above procedure and well dispersed in the AcEt solvent mixture. The image shows that the particles are crystalline with an approximate mean particle size of 2 nm. A histogram of the particle size distribution of the dispersed Pt nanoparticles is shown in Figure 2(b). The data was collected by measuring and recording the particles sizes of 51 particles from eight SEM images by hand.

Figure 2(c) shows the XRD pattern for the dispersed Pt nanoparticles. The 2θ peaks of 39.1°, 45.6°, 66.6° and 81.5° in Figure 2(c) are indicative of face centred cubic (fcc) platinum, with the lattice planes for the peaks corresponding to the (111), (200), (220) and (311) planes, respectively. The mean particle diameter, calculated from the XRD spectrum, Figure 2(c), using the Sherrer equation, is 2.2 nm which was in close agreement with the HRTEM results.

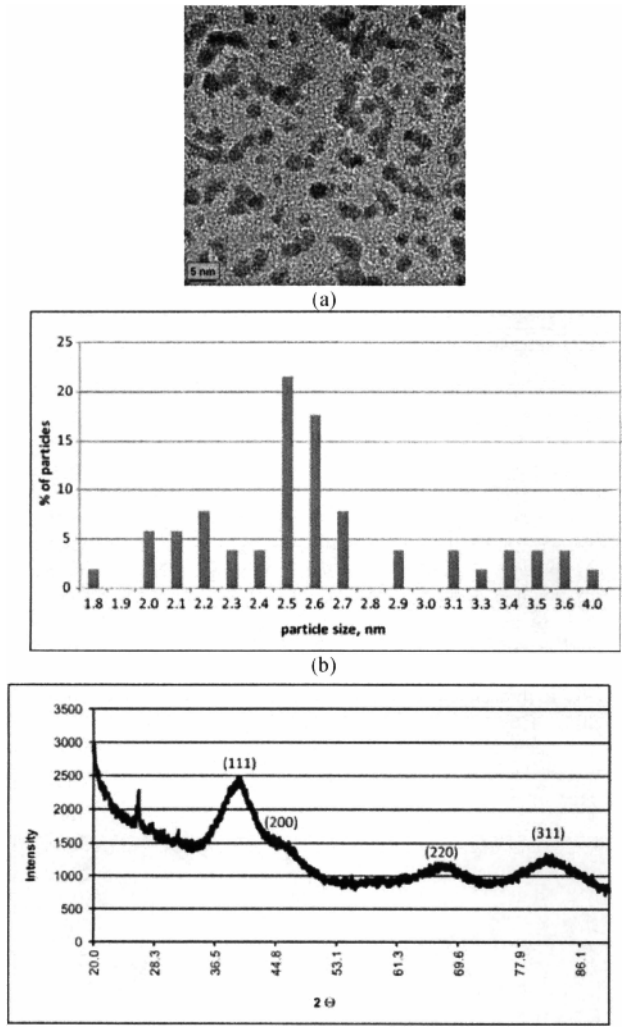

Figure 2. Imaging and properties of the Pt nanoparticles synthesised: (a) HRTEM image, (b) particle size distribution measured from HRTEM image, and (c) XRD pattern.

EPD of the Pt Nanoparticles onto the Copper Foil Electrodes

The data gathered in the EPD trials was plotted in Figure 3 as deposition flux with respect to deposition time for each applied voltage.

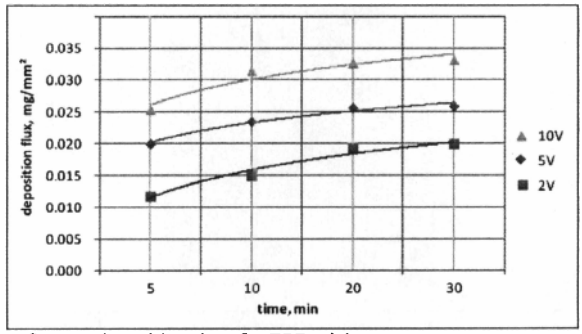

Figure 3. Deposition flux vs. deposition time for EPD trials.

Looking at the graph in Figure 3, the slope of each curve at each applied voltage appears to be similar for all the applied voltages, hence the polarization of the electrode in this system is assumed to be linear for the potential window of 2 – 10 V.

By inspecting the deposits with the naked eye, only the deposits prepared with an applied voltage of 5 V or higher appeared to cover the entire surface of the electrode in contact with the dispersion. Using SEM analysis, performed with a ZEISS EVO MA15VP scanning electron microscope, the thinnest and most uniform film was obtained by running the EPD process at an applied potential of 5 V for 5 minutes. Figure 4(a) shows the SEM image of the deposit prepared on a copper electrode by EPD for 5 minutes at an applied voltage of 5 V. The effect of lowering the dispersion concentration was studied by diluting the dispersion. This was achieved by adding 100 ml of acetone to 100 ml of the prepared dispersion, effectively reducing the Pt concentration in the dispersion to 0.9 g/l. By reducing the amount of ethanol in the solvent mixture as well as the concentration of platinum nanoparticles in dispersion, the deposition flux was further lowered without affecting the uniformity of the deposit significantly, as shown in Figure 4(b). The deposition time was doubled for the diluted dispersion to ensure a continuous platinum film was formed on the copper surface. As the deposition with the diluted dispersion for 10 minutes at 5V gave the best result, these parameters were used to prepare electrodes for the sintering analysis.

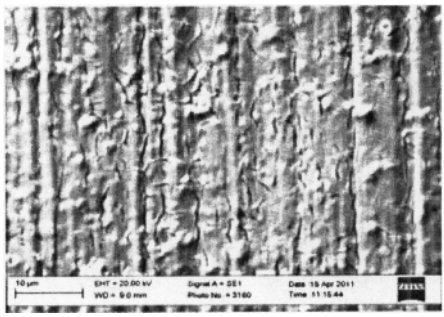

(a)

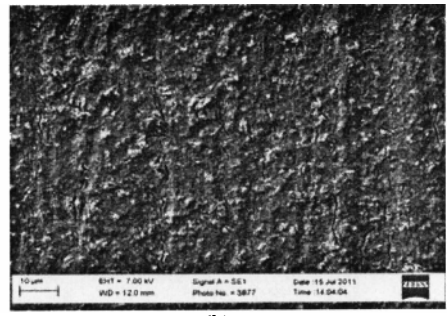

(b)

Figure 4. SEM of Pt deposit on copper electrode after EPD for (a) 5 minutes at 5 V with undiluted dispersion, and for (b) 10 minutes at 5 V with the diluted dispersion.

Sintering of the Pt Deposits

The sintered deposits were analysed by SEM, EDX, XRD, and HRTEM. The microstructure in each of the deposits was investigated using a ZEISS EVO MA15VP scanning electron microscope. Figure 5 shows representative images for each sintered sample.

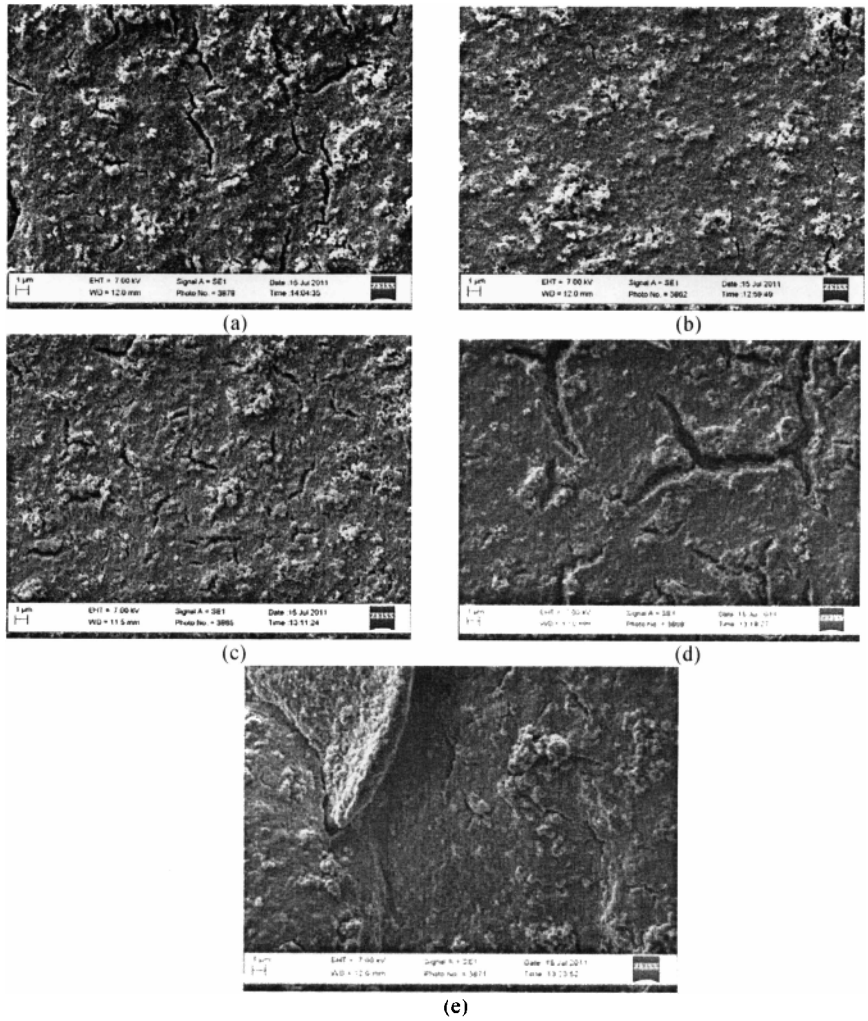

Figure 5. SEM images of Pt deposited on copper electrodes (a) at 25°C, unsintered, and after sintering at (b) 100°C, (c) 200°C, (d) 300°C, and (e) 400°C, in argon for 15 minutes each.

The cracks in the deposit before sintering, as seen in Figure 5(a), disappeared after sintering at 100°C, Figure 5(b), suggesting that the deposited particles were mobile on the copper surface. Both the HRTEM and XRD data indicate no significant change in the mean particle size of the platinum nanoparticles. Table 2 shows the XRD and HRTEM measurements of the mean particle sizes in the deposits.

Table II. XRD and HRTEM measurements of the mean particle size in the deposits

Sintering Temperature (°C)	Mean particle size: HRTEM (nm)	Particle size variation: HRTEM (nm)	Mean particle size: XRD Scherrer (nm)
25	2.5	1.8 - 4.0	2.56
100	2.8	2.0 - 4.0	2.52
200	3.9	2.5 - 5.0	3.96
300	43	2.5 - 150.0	11.72
400	100	10.0 - 600.0	13.83

The XRD spectrum, Figure 6, for the deposit sintered at 100°C also shows that no shift in the d-spacing for the platinum crystal planes has taken place since there is no shift in the 2θ values for the Pt peaks. Hence no alloying between the platinum deposit and the copper electrode had taken place after heating at 100°C.

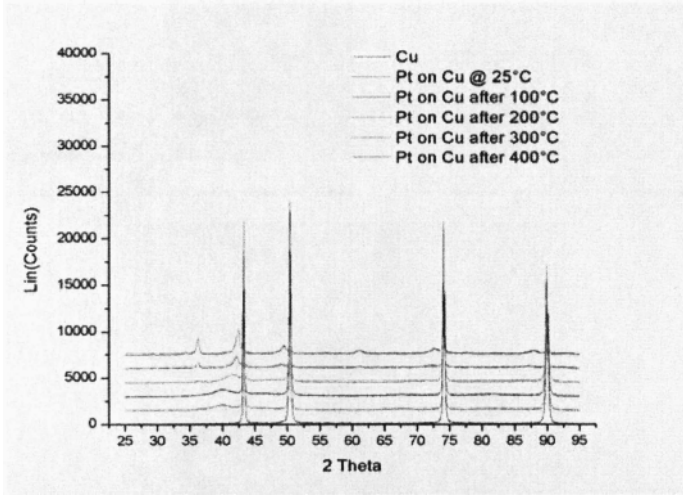

Figure 6. XRD spectra for the copper electrodes as well as the Pt deposits prepared by EPD on the copper electrodes.

HRTEM imaging of the platinum deposit after sintering at 100°C, Figure 7(b), indicates that no necking between the platinum nanoparticles had occurred at 100°C. Therefore, it can be concluded that no significant surface diffusion was taking place between the particles. The disappearance of the cracks

in the deposit can be attributed to settling of the Pt nanoparticles as the residual solvent and water evaporated from the deposit.

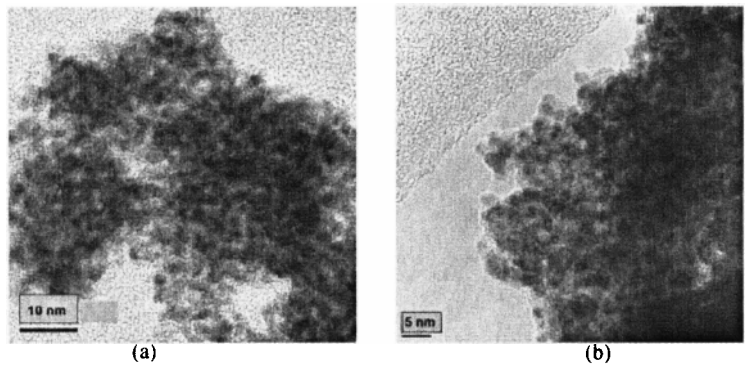

(a) (b)

Figure 7. HRTEM image of Pt deposit scraped off the copper electrode (a) before sintering, and (b) after sintering at 100°C.

Fine cracks reappeared on the deposit surface after sintering at 200°C, shown in Figure 5(c). This was indicated the formation of a densification gradient between the deposit and the copper surface, as well as immobilization of the deposit due to bonding with the copper substrate. In other words, sintering of the platinum nanoparticles must have begun at this temperature. Furthermore, the shift in the 2θ value for the [111] peak in the XRD spectrum of the platinum deposit from 40.0° to 41.6° is indicative of a decrease in the d-spacing of the [111] planes for the platinum phase indicating the onset of alloying. The other peaks had signals which were too weak to be detected. The mean particle size from both the XRD and HRTEM data, Figure 6 and Figure 8(a), was calculated to be 3.9 nm in both cases, indicating that very little coarsening had occurred. Densification of the deposit was occurring dominantly via surface diffusion at this temperature.